Journal of Molecular Structure 1231 (2021) 129943

Contents lists available at ScienceDirect

Journal of Molecular Structure

journal homepage: www.elsevier.com/locate/molstr

# Synthesis and *in silico* studies of Novel Ru(II) complexes of Schiff base derivatives of 3-[(4-amino-5-thioxo-1,2,4-triazole-3-yl)methyl]-2(3H)-benzoxazolone compounds as potent Glutathione S-transferase and Cholinesterases Inhibitor

Ragip Adiguzel[a,b,c], Fikret Türkan[d,*], Ümit Yildiko[e], Abdülmelik Aras[f], Enes Evren[g], Tijen Onkol[h]

[a] Department of Chemistry and Chemical Process Technologies/Laboratory Technology Program, Vocational School of Tunceli, Munzur University, 62000 Tunceli, Turkey
[b] Head of Department of Chemical Technologies in Institute of Graduate Studies, Munzur University, 62000 Tunceli, Turkey
[c] Rare Earth Elements Research and Application Center, Munzur University, 62000 Tunceli, Turkey
[d] Health ServicesVocational School, Igdır University, Igdır, Turkey
[e] Department of Biochemistry, Faculty of Science and Letters Igdir University, 76000 Igdır, Turkey
[f] Architecture and Engineering Faculty, Department of Bioengineering, Kafkas University, Kars, Turkey
[g] Catalysis Research and Application Center, Inonu University, 44280Malatya, Turkey
[h] Gazi University, Faculty of Pharmacy, Department of Pharmaceutical Chemistry, 06330 Ankara, Turkey,

ARTICLE INFO

*Article history:*
Received 20 October 2020
Revised 7 January 2021
Accepted 10 January 2021
Available online 13 January 2021

*Keywords:*
2(3H)-benzoxazolone
4-amino-5-thioxo-1,2,4-triazole
Schiff base
Ruthenium complexesy
Enzyme inhibition
Docking

ABSTRACT

Novel Ru(II) complexes of Shiff base derivatives of 3-[(4-amino-5-thioxo-1,2,4-triazole-3-yl)methyl]-2(3*H*)-benzoxazolone were synthesized. The ligands (1a-e) were confirmed by IR, $^{1}$H NMR, and $^{13}$C NMR spectra (only 1b and 1c). Structures of the synthesized Ru(II) complexes (2a-e) were illuminated by elemental analysis, IR, $^{1}$H NMR, $^{13}$C NMR, and mass spectra. As the biological studies, the inhibitory potency of the ligands and the novel synthesized complexes were evaluated against the glutathione S-transferase (GST), acetylcholinesterase (AChE) and butyrylcholinesterase (BChE) enzymes in vitro conditions. Ki values in the range of 26.87-47.63 µM for AChE, 23.51-42.81 µM for BChE, and 33.14-51.73 µM for GST, respectively. The free binding energy of most active inhibitors against AChE, BChE, and GST enzymes were detected as -10.183 kcal/mol, -9.111 kcal/mol, and -6.097 kcal/mol, respectively. All compounds docked were observed to bind in the active site of the enzymes with similar binding orientation and binding interactions with the surrounding amino acids.



## 1. Introduction

Schiff bases are organic compounds that have an important position as ligands in metal coordination chemistry since their discovery. They can form stable complexes with some transition metals including rare-earth metals [1-3]. Schiff bases containing nitrogen, oxygen, and sulfur donor atoms have great importance for biological systems due to their ability to illuminate the mechanism of reactions such as transformation [4-6]. There are various biological activities of the 1,2,4-triazole Schiff bases such as antioxidant, antitumor, antimicrobial, antitubercular [7], anti-inflammatory, antipyretic, antifungal, and antibacterial [8]. Hence, the application of their effects on functional materials, agrochemicals, and pharmaceuticals is becoming more important [9].

The importance of sulphonamide Schiff bases for the design of enzyme inhibitors has been demonstrated in the literature [10]. Therefore, herein Glutathione S-transferases (GST), acetylcholinesterase (AChE), and butyrylcholinesterase (BChE) enzymes were examined regarding the inhibitory activity. Acetylcholinesterase enzymes belong to the hydrolase class and are encoded by chromosomes 7 [11]. They are used as the target of drugs in the treatment of some diseases, including Alzheimer's disease (AD) [9]. The biological responsibility of the AChE is to swiftly terminate the neural impulse transmission in the synaptic cleft by hydrolysis of the ACh to acetate and choline [12-14].

Butyrylcholinesterase (BChE) accepted as a standard approach synthesized in the liver is used in the symptomatic treatment

* Corresponding author.
*E-mail address:* fikret.turkan@igdir.edu.tr (F. Türkan).

https://doi.org/10.1016/j.molstruc.2021.129943
0022-2860/

of neurodegenerative diseases [15]. BChE with three-dimensional-structures is a serine hydrolase related to AChE. Their catalytic mechanisms are close, however, substrate specificity and inhibitor sensitivity are different. Unlike AChE, which enables acetylcholine to terminate the effect of acetylcholine in the cholinergic system, studies have not demonstrated direct participation of BChE in the cholinergic system [16,17].

Glutathione S-transferase (GST) enzyme family located in the liver plays an important role in detoxification and takes part in the process of adding glutathione to oxidative stress products [18,19]. However, to maintain their survival and obtain drug resistance this feature is similarly used by cancer cells. Therefore, various members of the GST enzyme were determined overexpressed in some types of cancers [20]. It has been determined that GST enzyme inhibitors eliminate drug resistance by sensitizing tumor cells to different anticancer drugs [21], and therefore inhibitory studies of this enzyme have gained more importance.

In this study, starting from the known fact that Shiff base derivatives of 3-[(4-amino-5-thioxo-1,2,4-triazole-3-yl)methyl]-2(3H)-benzoxazolone have various biological activities [7,8], we synthesized new Ruthenium(II) complexes of Shiff base derivatives of 3-[(4-amino-5-thioxo-1,2,4-triazole-3-yl)methyl]-2(3H)benzoxazolone. We determined some metabolic enzyme inhibitory effects of these compounds.Besides, the molecular docking study was carried out to observe enzyme inhibitor interaction.

## 2. Experimental section

### 2.1. Materials and methods

All chemicals were acquired from commercial firms that are concerning chemicals, without further purification. The starting materials necessary for the synthesis of ligands were available in our laboratory. From the solvents, only toluene that was used during the synthesis of Ru(II) complexes (2a-e) was purified by distillation over the drying agents indicated and was transferred to the reaction media under argon. $[Ru(p\text{-cymene})Cl_2]_2$ compounds were purchased from Sigma Aldrich Co. (Dorset, UK). Melting points were determined using the Electrothermal 9100 melting point detection apparatus in capillary tubes and the melting points are reported as uncorrected values. Elemental analyses were carried out with a Leco CHNS–O model 932 elemental analyzer at Inonu University, Malatya, Turkey. FT-IRspectra of the Ru(II) complexes (2a-e) were recorded using a JASCO 6700 spectrophotometer in the wavenumber range of 4000–400 $cm^{-1}$ at Munzur University, Tunceli, Turkey. All spectra represented 32 scans and resolution 4 $cm^{-1}$. $^1H$ NMR and $^{13}C$ NMR data were obtained in DMSO-$d_6$ solvent on a Bruker AVANCE 400 spectrometer at room temperature, at Inonu University, Malatya, Turkey. The high-resolution mass spectra (HRMS) were obtained on a Waters LCT Premier XE Mass Spectrometer also coupled to an EQUITY Ultra Performance Liquid Chromatography System at Faculty of Pharmacy, Gazi University, Ankara, Turkey.

### 2.2. Design and synthesis of the ligands (1a-e)

3-[(*o*/*p*-substitutedphenylmethylidene]amino-5-thioxo-1,2,4-triazol-3-yl)methyl]-2(3H)-benzoxazolone(1a-e) which are Shiff base derivatives of 3-[(4-amino-5-thioxo-1,2,4-triazole-3-yl)methyl]-2(3*H*)-benzoxazolone were synthesized by using microwave technique as shown in Scheme 1, according to given method in the literature. The structures of the synthesized ligands (1a-e) were checked out by IR, $^1H$ NMR, and $^{13}C$ NMR spectra. $^{13}C$ NMR spectra data of the ligands (1b and 1c) were obtained firstly in our current study.

#### 2.2.1. Spectral results for ligands

**1a:** FT-IR $\nu$ (cm-1), 3230, 1776, 1484, 1236; $^1H$ NMR (DMSO-$d_6$) $\delta$ 14.10 (1H, s, NH), 10.01 (1H, s, N=CH), 7.16-7.85 (8H, m, Ar-H), 5.30 (2H, s, $CH_2$);

**1b:** FT-IR $\nu$ (cm-1), 3248, 1744, 1480, 1269; $^1H$ NMR (400 MHz DMSO-$d_6$) $\delta$(ppm): 14.17 (1H, s, NH), 10.82 (1H, s, N=CH),7.14-8.14 (8H, m, Ar-H), 5.34 (2H, s, $CH_2$); $^{13}C$ NMR $^{13}C\{^1H\}$ NMR (100 MHz, DMSO-$d_6$) $\delta$ (ppm):162.6 (**C**=S), 159.5 (**C**=O), 146.5 (N**C**H(o-$BrC_6H_4$)), 110.2, 110.3, 123.2, 124.5, 126.1, 128.7, 131.1, 131.8, 134.0, 134.7, 142.4 (Ar-C) of NCH(o-$BrC_6H_4$) and $CCH_2NC(\mathbf{C}_6H_4)$ in either benzene ring, 153.8 ($N\mathbf{C}CH_2$), 37.4 ($NC\mathbf{C}H_2$).

**1c:** FT-IR $\nu$ ($cm^{-1}$), 3258, 1759, 1462, 1265.; $^1H$ NMR (400 MHz, DMSO-$d_6$) $\delta$ (ppm): 14.12 (1H, s, NH), 10.06 (1H, s, N=CH), 7.13-7.81 (8H, m, Ar-H), 5.30 (2H, s, $CH_2$); $^{13}C\{^1H\}$ NMR (100 MHz, DMSO-$d_6$) $\delta$ (ppm): 162.6 (**C**=S), 162.4 (**C**=O),

146.1 (N**C**H(p-$BrC_6H_4$)), 110.1, 110.3, 123.2, 124.5, 126.9, 130.9, 131.0, 131.6, 132.7, 142.3 (Ar-C) of NCH(o-Br$\mathbf{C}_6H_4$) and $CCH_2N(\mathbf{C}_6H_4)$ in either benzene ring, 153.8 ($N\mathbf{C}CH_2$), 37.4 ($NC\mathbf{C}H_2$).

**1d:** FT-IR $\nu$ ($cm^{-1}$), 3238, 1748, 1482, 1242; $^1H$ NMR (DMSO-$d_6$) $\delta$ (ppm): 14.10 (1H, s, NH), 10.01 (1H, s, N=CH), 7.16-7.85 (8H, m, Ar-H), 5.30 (2H, s, $CH_2$);

**1e:** 3298, 1744, 1484, 1241; $^1H$ NMR (DMSO-$d_6$) $\delta$ (ppm): 14.06 (1H, s, NH), 10.06 (1H, s, N=CH), 7.17-7.88 (8H, m, Ar-H), 5.30 (2H, s, $CH_2$)

### 2.3. Design and synthesis of the Ru(II) complexes (2a-e)

All the Ru(II) complexes benzoxazolone-based ligands (1a-e) were prepared under the argon gas atmosphere.

#### 2.3.1. Synthesis of novel Ru(II) complexes (2a-e)

The ligands 1a-e (0.122 mmol), $[Ru(p\text{-cymene})Cl_2]_2$ (0.122 mmol) and dry PhMe solvent (7 mL), was added in a schlenk flask (50 mL) The mixture was stirred for 2 h at 70 °C and then the brick-colored mixture was stirred for 20 h at 95 °C. After the reaction was finished, PhMe was removed under vacuum. The crude product was crystallized in $CH_2Cl_2/C_2H_5)_2O$ (1:3 v/v) and yellow-brown $RCl_2L(\eta^6$-p-cymene) 2a, 2c-e were obtained. Since enough precipitate formed, only 2b complex was directly washed with $C_2H_5)_2O$ and dried in a vacuum.The crude precipitate was crystallized in a $CH_2Cl_2/C_2H_5)_2O$, because in the complexes (2a, 2c-e) weren't formed sufficient precipitate.

**2a:** Yield: 78%, mp >225°C. Elemental Analysis (EA): Calcd for $C_{27}H_{27}Cl_2N_5O_2SRu$ (656.97): C, 49.31%; H, 4.11%; N, 10.65%; S, 4.87%. Found: C, 48.87%; H, 4.25%; N, 10.32%; S, 5.17%. FT-IR $\nu$ ATR ($cm^{-1}$) 3197 N-H, 3050 C-H arom., 3028 H-C=N, 2965 asym. C-H, 2934 sym. C-H, 1779 C=O, 1609,1589 C=N, 1482 C=C, 1361 C-H(bend),1235 C=S, 586 Ru-N. $^1H$ NMR (400 MHz, $CDCl_3$) $\delta$ (ppm): 13.12 (1H, s, NH), 9.62 (1H, s, N=CH), 7.02-7.91 (9H m, Ar-H of NCH($C_6\boldsymbol{H}_5$) and $CCH_2N(C_6\boldsymbol{H}_4)$), 5.26-5.45 (4H d, Ru-$C_6\boldsymbol{H}_4$), 5.20 (2H, s, $CH_2$); 3.02(1H h, Ru-$C_6H_4C\boldsymbol{H}(CH_3)_2$; 2.26 (3H s, Ru-$C_6H_4C\boldsymbol{H}_3$); 1.33 (6H d, Ru-$C_6H_4CH(C\boldsymbol{H}_3)_2$. $^{13}C$ NMR $^{13}C\{^1H\}$ NMR (100 MHz, $CDCl_3$) $\delta$ (ppm): 164.2 (**C**=S), 160.3 (**C**=O); 145.6 (N**C**H($C_6H_5$)); 109.3, 110.1, 123.3, 124.4, 128.2, 129.2, 129.5, 129.7 131.1, 133.5, 134.3 142.3 (Ar-C) of NCH($\boldsymbol{C}_6H_5$) and $CCH_2N(\boldsymbol{C}_6H_4)$ in either benzene ring; 153.6 ($N\boldsymbol{C}CH_2$); 82.1, 83.5, 98.8, 103.7 Ru-$\boldsymbol{C}_6H_4CH(CH_3)_2$; 36.5 $C\boldsymbol{C}H_2N$;30.6 Ru-$C_6H_4\boldsymbol{C}H(CH_3)_2$; 22.2 Ru-$C_6H_4CH(\boldsymbol{C}H_3)_2$; 18.4 Ru-$C_6H_4\boldsymbol{C}H_3$. ESI-MS (positive mode, m/z): calcd 586.07, found 586.08 for $[M\text{-}2Cl]^{2+}$.

**2b:** Yield: 84%, mp >235°C. Elemental Analysis (EA): Calcd for $C_{27}H_{26}BrCl_2N_5O_2SRu$ (735.97): C, 44.02%; H, 3.53%; N, 9.51%; S, 4.34%. Found: C, 43.55%; H, 3.69%; N, 9.23%; S, 4.48%. FT-IR $\nu$ ATR ($cm^{-1}$) 3176 N-H, 3058 C-H arom., 3029 H-C=N, 2959 asym. C-H, 2936 sym. C-H, 1785 C=O, 1609, 1584 C=N, 1480 C=C, 1336 C-H(bend), 1237 C=S, 749 C-Br, 590 Ru-N. $^1H$ NMR (400 MHz, $CDCl_3$) $\delta$ (ppm): 13.09 (1H, s, NH), 10.38 (1H, s, N=CH), 7.06-8.36 (8H m,

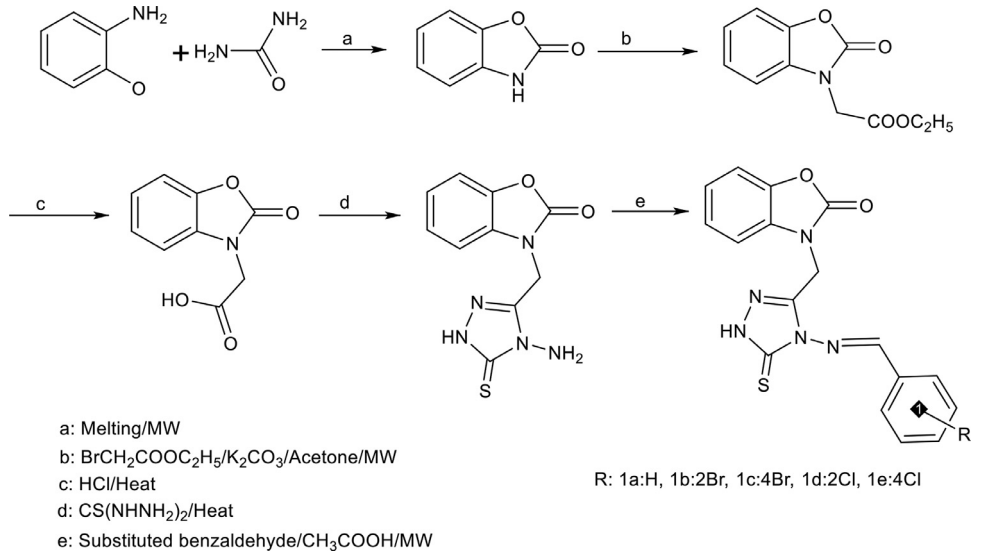


**Schema 1.** Synthesis steps of the ligands 3-[(*o*/*p*-substitutedphenylmethylidene]amino-5-thioxo-1,2,4-triazol-3-yl)methyl]-2(3H)-benzoxazolone (1a-e).

Ar-H of NCH(o-Br$C_6\boldsymbol{H}_4$) and $CCH_2N(C_6\boldsymbol{H}_4)$), 5.26-5.47 (4H d, Ru-$C_6\boldsymbol{H}_4$), 5.23 (2H, s, $CH_2$); 3.05(1H h, Ru-$C_6H_4C\boldsymbol{H}(CH_3)_2$; 2.28 (3H s, Ru-$C_6H_4C\boldsymbol{H}_3$); 1.34 (6H d, Ru-$C_6H_4CH(C\boldsymbol{H}_3)_2$. $^{13}C\{^1H\}$ NMR (100 MHz, $CDCl_3$) $\delta$ (ppm): 164.7 (**C**=S), 160.3 (**C**=O); 145.8 (N**C**H(o-Br$C_6H_4$)), 109.5, 110.1, 123.3, 124.5, 126.8, 128.4, 129.2, 129.7,130.7 133.4, 134.4, 142.3 (Ar-C) of NCH(o-Br$\boldsymbol{C}_6H_4$) and $CCH_2N(\boldsymbol{C}_6H_4)$ in either benzene ring; 153.6 (N**C**$CH_2$); 82.1, 83.9, 98.9, 103.8 Ru-$\boldsymbol{C}_6H_4CH(CH_3)_2$; 36.5 C**C**$H_2$N;30.6 Ru-$C_6H_4\boldsymbol{C}H(CH_3)_2$; 22.3 Ru-$C_6H_4CH(\boldsymbol{C}H_3)_2$; 18.4 Ru-$C_6H_4\boldsymbol{C}H_3$. ESI-MS (positive mode, m/z): calcd 664.97, found 664.49 for $[(M-2Cl)]^{2+}$.

**2c:** Yield: 81%, mp >300°C. Elemental Analysis (EA): Calcd for $C_{27}H_{26}BrCl_2N_5O_2SRu$ (735.97): C, 44.02%; H, 3.53%; N, 9.51%; S, 4.34%. Found: C, 43.54%; H, 3.64%; N, 9.33%; S, 4.45%. FT-IR $\nu$ ATR ($cm^{-1}$) 3172 N-H, 3051 C-H arom., 3021 H-C=N, 2967 asym. C-H, 2929 sym. C-H, 1775 C=O, 1609, 1584 C=N, 1480 C=C, 1361 C-H(bend), 1235 C=S, 747 C-Br, 588 Ru-N. $^1H$ NMR (400 MHz, $CDCl_3$) $\delta$ (ppm): 13.16 (1H, s, NH), 9.65 (1H, s, N=CH), 7.03-8.7.79 (8H m, Ar-H of NCH(p-Br$C_6\boldsymbol{H}_4$) and $CCH_2N(C_6\boldsymbol{H}_4)$), 5.26-5.45 (4H d, Ru-$C_6\boldsymbol{H}_4$), 5.19 (2H, s, $CH_2$); 3.01 (1H h, Ru-$C_6H_4C\boldsymbol{H}(CH_3)_2$; 2.31 (3H s, Ru-$C_6H_4C\boldsymbol{H}_3$); 1.33 (6H d, Ru-$C_6H_4CH(C\boldsymbol{H}_3)_2$. $^{13}C\{^1H\}$ NMR (100 MHz, $CDCl_3$) $\delta$ (ppm):162.4 (**C**=S), 160.4 (**C**=O); 145.6 (N**C**H(p-Br$C_6H_4$)), 109.4, 110.1, 123.3, 124.4, 125.3, 128.2, 128.6 129.0, 129.6, 130.0 130.8, 132.6 (Ar-C) of NCH(p-Br$\boldsymbol{C}_6H_4$) and $CCH_2N(\boldsymbol{C}_6H_4)$ in either benzene ring; 153.6 (N**C**$CH_2$); 82.1, 83.9, 98.9, 103.8 Ru-$\boldsymbol{C}_6H_4CH(CH_3)_2$; 36.5 C**C**$H_2$N;30.6 Ru-$C_6H_4\boldsymbol{C}H(CH_3)_2$; 22.2 Ru-$C_6H_4CH(\boldsymbol{C}H_3)_2$; 18.4 Ru-$C_6H_4\boldsymbol{C}H_3$. ESI-MS (positive mode, m/z): calcd 664.97 found 664.99 for $[M-2Cl]^{2+}$.

**2d:** Yield: 83%, mp >233°C. Elemental Analysis (EA): Calcd for $C_{27}H_{26}Cl_3N_5O_2SRu$ (691.42): C, 46.86%; H, 3.76%; N, 10.12%; S, 4.62%. Found: C, 46.37%; H, 3.62%; N, 9.66%; S, 4.18%. FT-IR $\nu$ ATR ($cm^{-1}$) 3169 N-H, 3049 arom. C-H, 3019 H-C=N, 2967 asym. C-H, 2924 sym. C-H, 1775 C=O, 1610, 1586 C=N, 1482 C=C, 1359 C-H(bend), 1235 C=S, 744 C-Cl, 586 Ru-N. $^1H$ NMR (400 MHz, CDCl3) $\delta$ (ppm): 13.16 (1H, s, NH), 9.63 (1H, s, N=CH), 7.03-7.79 (8H m, Ar-H of NCH(o-Cl$C_6\boldsymbol{H}_4$) and $CCH_2N(C_6\boldsymbol{H}_4)$), 5.26-5.45 (4H d, Ru-$C_6\boldsymbol{H}_4$), 5.20 (2H, s, $CH_2$); 2.99 (1H h, Ru-$C_6H_4C\boldsymbol{H}(CH_3)_2$; 2.26 (3H s, Ru-$C_6H_4C\boldsymbol{H}_3$); 1.33 (6H d, Ru-$C_6H_4CH(C\boldsymbol{H}_3)_2$. $^{13}C\{^1H\}$ NMR (100 MHz, $CDCl_3$) $\delta$ (ppm): 162.3 (**C**=S), 160.4 (**C**=O); 145.6 (N**C**H(o-Cl$C_6H_4$)), 109.4, 110.1, 123.3, 124.4, 125.3, 128.6, 130.4, 130.7, 131.9, 132.6, 134.5, 142.3 (Ar-C) of NCH(o-Cl$\boldsymbol{C}_6H_4$) and $CCH_2N(\boldsymbol{C}_6H_4)$ in either benzene ring; 153.6 (N**C**$CH_2$); 82.1, 83.5, 98.9, 103.8 Ru-$\boldsymbol{C}_6H_4CH(CH_3)_2$; 36.5 C**C**$H_2$N;30.6 Ru-$C_6H_4\boldsymbol{C}H(CH_3)_2$; 22.2 Ru-$C_6H_4CH(\boldsymbol{C}H_3)_2$; 18.4 Ru-$C_6H_4\boldsymbol{C}H_3$. ESI-MS (positive mode, m/z): calcd 709.42, found 709.02 for $[M+NH_4]^+$.

**2e:** Yield: 80%, mp >300°C. Elemental Analysis (EA): Calcd for $C_{27}H_{26}Cl_3N_5O_2SRu$ (691.42): C, 46.86%; H, 3.76%; N, 10.12%; S, 4.62%. Found: C, 46.39%; H, 4.02%; N, 9.69%; S, 4.71%. FT-IR $\nu$ ATR ($cm^{-1}$) 3220 N-H, 3051 arom. C-H,3021 H-C=N, 2965 asym. C-H, 2927 sym. C-H, 1772 C=O, 1609, 1592 C=N, 1483 C=C, 1361 C-H(bend), 1235 C=S, 744 C-Cl, 586 Ru-N. $^1H$ NMR (400 MHz, CDCl3) $\delta$ (ppm): 13.16 (1H, s, NH), 9.65 (1H, s, N=CH), 7.03-7.86 (8H m, Ar-H of NCH(p-Cl$C_6\boldsymbol{H}_4$) and $CCH_2N(C_6\boldsymbol{H}_4)$), 5.26-5.45 (4H d, Ru-$C_6\boldsymbol{H}_4$), 5.20 (2H, s, $CH_2$); 3.01 (1H h, Ru-$C_6H_4C\boldsymbol{H}(CH_3)_2$; 2.26 (3H s, Ru-$C_6H_4C\boldsymbol{H}_3$); 1.33 (6H d, Ru-$C_6H_4CH(C\boldsymbol{H}_3)_2$. $^{13}C\{^1H\}$ NMR (100 MHz, $CDCl_3$) $\delta$ (ppm): 162.4 (**C**=S), 160.3 (**C**=O); 145.6 (N**C**H(p-Cl$C_6H_4$)), 109.4, 110.1, 123.3, 124.5, 128.4,129.6, 130.7, 131.8, 132.6, 138.3,139.9 142.3 (Ar-C)of NCH(p-Cl$\boldsymbol{C}_6H_4$) and $CCH_2N(\boldsymbol{C}_6H_4)$ in either benzene ring; 153.6 (N**C**$CH_2$); 82.1, 83.6, 98.9, 103.8 Ru-$\boldsymbol{C}_6H_4CH(CH_3)_2$; 36.6 C**C**$H_2$N;30.6 Ru-$C_6H_4\boldsymbol{C}H(CH_3)_2$; 22.3 Ru-$C_6H_4CH(\boldsymbol{C}H_3)_2$; 18.4 Ru-$C_6H_4\boldsymbol{C}H_3$. ESI-MS (positive mode, m/z): calcd 620.52, found 620.05 for $[M-2Cl]^{2+}$.

### *2.4. Enzyme inhibitory activity*

#### *2.4.1. Determination of AChE and BChE inhibitory activity*

The determination of cholinesterase activity was done by the Ellman method with some change [22,23]. For BChE and AChE inhibitions test butyrylthiocholine iodide and acetylthiocholine iodide were used as substrates. To determine enzyme activities three solutions of 50 µL BChE-AChE, 5,5′-Dithiobis(2-nitrobenzoic acid) (DTNB), 100 µL tris/HCl buffer solution (1 mM, pH 8.0), and drug solution (10 mL) was stirred and then left in the dark at room temperature for 10 minutes. Finally, 0.5 mM, 50 µL of 2-nitrobenzoic (5,5-Dithiobis acid) was added to the prepared mixture, and the reaction was initiated. By the formation of DTNB color change was calculated at 412 nm by UV–Vis spectrophotometer [24].

#### *2.4.2. Determination of GST inhibitory activity*

Novel Ru(II) complexes of Shiff base derivatives of 3-[(4-amino-5-thioxo-1,2,4-triazole-3-yl)methyl]-2(3H)-benzoxazolone inhabitation effects were determined in the range of 20-100 µM concentration on GST enzyme activity according to the to (Habig et al. 1974) previous publications [25,26]. Their Ki

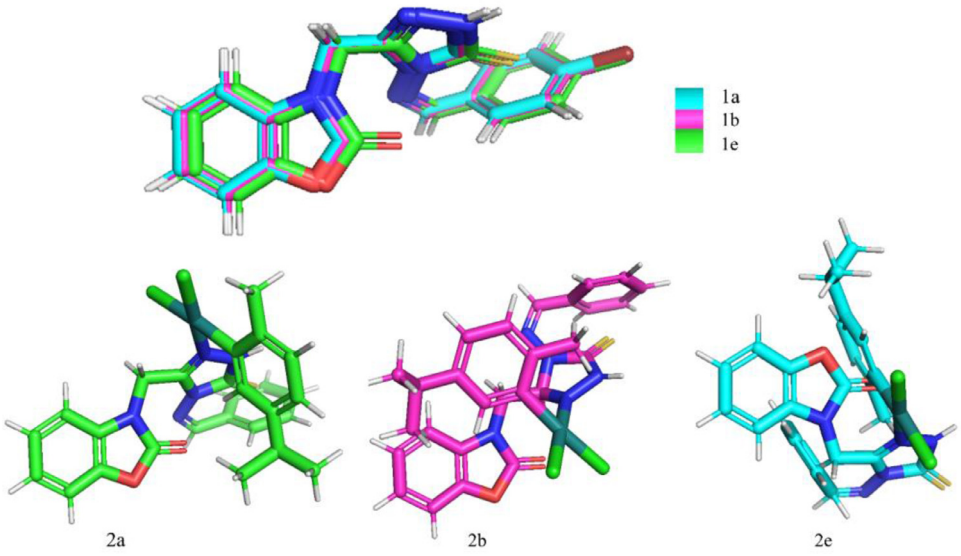


**Fig. 1.** Optimized 3D structures of the Shiff base derivatives and Ru(II) complexes ligands.

and $IC_{50}$ values were calculated and results were given in Table 1.

### 2.5. Molecular docking studies

In the molecular docking study, acetylcholinesterase (PDB ID: 6O4W) [27], butyrylcholinesterase (PDB ID: 6SAM) [28], and glutathione s-transferase (PDB ID: 5JCU) [29]. enzymes were used as receptors. Crystallographic structures of enzymes obtained from the protein database (PDB) at the Research Collaboratory for Structural Bioinformatics (RCSB) (see http//www.rcsb.org/pdb). The Maestro Molecular Modeling platform (version 11.8) of the Schrödinger, LLC model was used as the docking program [30]. The structures of the ligands that were papered with ChemBio3D is part of the ChemBioOffice 2019 Suite in SDF file format as 3D structures (Fig. 1). The ionization is created by removing or adding protons from the ligand. Ionization work can be quite useful for generating a varied range of ionization filled with a chosen pH range. In the Ligand optimization, the force field geometry is optimized in the protein, and partial atomic loads are perfectly presented using the force field. During the enzymatic process, it is very important to evaluate the changes in the protonation status of functional groups at the right time and to elucidate the proton addition mechanism. The Missing residues or atoms fixes by the program. Water molecules play an important role in ligand binding. It should be classified according to their interactions with neighboring protein atoms and water molecules. When the right water molecules are targeted and removed, significant gains in affinity and selectivity are obtained [31] Lig prep, Protein Preparation Wizard, and Receptor Grid Generation modules of Maestro software, at this stage all water molecules were removed and polar hydrogen atoms were added. A grid box was formed around the active site of the proteins containing natural ligands. These studies were carried out according to the methods used in the previous studies [32,33]. The Glide score and energy were analyzed for receptor binding affinity and the interactive nature of the Ligand - proteins. Molecular docking studies were performed with the Glide docking module under Maestro. The resulting receptor model, 2D, and 3D interactions were visualized with Maestro and Discovery Studio 2017 version [34].

## 3. Results and discussion

### 3.1. Experimental

Characteristic peaks of the ligands in the IR spectrum (1a-e) were confirmed with values are given in literature The structures of the synthesized Ru(II) complexes (2a-e) were illuminated by elemental analysis, IR, $^{1}H$ NMR, $^{13}C$ NMR, and mass spectra (See Fig. 2). According to mass spectra and elemental analyses, the general formula of all complexes was determined as [Ru($\eta^6$-p-cymene)$LCl_2$].

#### 3.1.1. IR spectra

The N-H stretching bands in the IR spectra of all ligands (1a-e) were observed at 3230, 3248, 3258, 3238, and 3298 $cm^{-1}$respectively[7]. These N-H stretching bands for Ru(II) complexes (2a-e) shifted to the low-frequency region and were observed at 3197, 3176, 3172, 3169, and 3220 $cm^{-1}$ respectively (2a-e). The shift to low wave number is compatible with decreasing electron density in the N-H bond [35,36], In other vibration frequencies of all complexes didn't appear a considerable change except the C=O stretching bands. In general, it is reported in the literature when the metal ion is coordinated by the C=O group, in contrast to results the C=O band shifts to the lower frequency region [37]. The reason for the shifting to the high frequency of the CO band (from 1744 to 1785 $cm^{-1}$) can be explained by the increase in electron density of the CO bond due to the coordination of nitrogen of triazole ring with the metal. On the other side, Ru-N vibration frequency has been reported that observed at about 700-416 $cm^{-1}$region in the literature [35,38,39]. As for in Ru(II) complexes synthesized by our research group Ru-N peak appeared between 586-590 $cm^{-1}$ as a mild intense band.

#### 3.1.2. NMR spectra

While in the $^{1}H$- NMR spectrum of ligands (1a-e), N-H proton over 1,2,4-triazole ring was observed at $\delta$=14.10, 14.17, 14.12, 14.10, and 14.06 ppm as a singlet peak respectively, this peak for Ru(II) complexes (2a-e) shifted to a lower frequency and was observed at observed between at $\delta$=13.09-13.16 ppm [7,40]. This shifting to lower frequency shows that around N-H proton over 1,2,4-triazole ring change. In this case, it can be explained over N atom in the 1,2,4-triazole ring with the coordination of metal. So all ligands acted as a monodentate ligand.

**Table 1**
The inhibition results of the Shiff base derivatives ligand (1a-e) (a) and Ru(II) complex (2a, e) (b) against glutathione S-transferase (GST), acetylcholinesterase (AChE), and butyrylcholinesterase (BChE) enzymes.

(a) Shiff base derivatives ligand (1a-e)

| Ligand Structures | $IC_{50}$ (μM) | | | | | | $K_i$ (μM) | | |
|---|---|---|---|---|---|---|---|---|---|
| | AChE | $R^2$ | BChE | $R^2$ | GST | $R^2$ | AChE | BChE | GST |
| 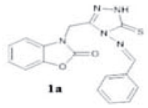 1a | 41.70 | 0.9491 | 30.14 | 0.9555 | 48.12 | 0.8821 | 37.88 | 23.51 | 40.07 |
| 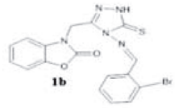 1b | 32.03 | 0.9603 | 40.10 | 0.9748 | 58.23 | 0.8627 | 30.25 | 35.78 | 47.54 |
| 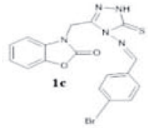 1c | 43.42 | 0.9606 | 36.79 | 0.9455 | 58.72 | 0.815 | 38.96 | 31.58 | 51.73 |
| 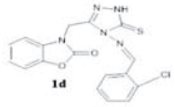 1d | 33.62 | 0.9712 | 43.63 | 0.9739 | 46.2 | 0.931 | 30.18 | 33.45 | 38.75 |
| 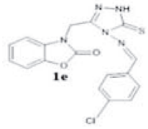 1e | 44.41 | 0.9432 | 45.05 | 0.9814 | 48.98 | 0.9582 | 41.13 | 40.09 | 38.76 |
| Tacrine | 7.80 | 0.9443 | 22.36 | 0.9628 | | | 8.77 | 19.73 | |

**(b) Ru(II) complex (2a, e)**

| Ru(II) complex Structures | $IC_{50}$ (μM) | | | | | | $K_i$ (μM) | | |
|---|---|---|---|---|---|---|---|---|---|
| | AChE | $R^2$ | BChE | $R^2$ | GST | $R^2$ | AChE | BChE | GST |
| 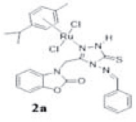 2a | 53.23 | 0.9817 | 40.99 | 0.9682 | 42,0 | 0.9315 | 47.63 | 29.74 | 33.14 |
| 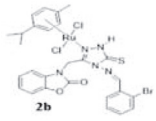 2b | 40.84 | 0.9656 | 32.78 | 0.9703 | 53.25 | 0.8976 | 33.91 | 26.33 | 46.72 |
| 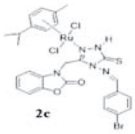 2c | 35.76 | 0.9574 | 40.46 | 0.9620 | 47.46 | 0.9414 | 26.87 | 31.11 | 39.04 |
| 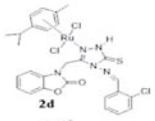 2d | 43.68 | 0.8989 | 50.46 | 0.9264 | 49.70 | 0.9937 | 34.04 | 42.81 | 42.78 |
| 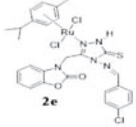 2e | 37.06 | 0.9231 | 43.59 | 0.9853 | 52.45 | 0.9742 | 27.78 | 36.19 | 44.47 |
| Tacrine* | 7.80 | 0.9443 | 22.36 | 0.9628 | | | 8.77 | 19.73 | |

* Used as a positive control for AChE and BChE enzymes.

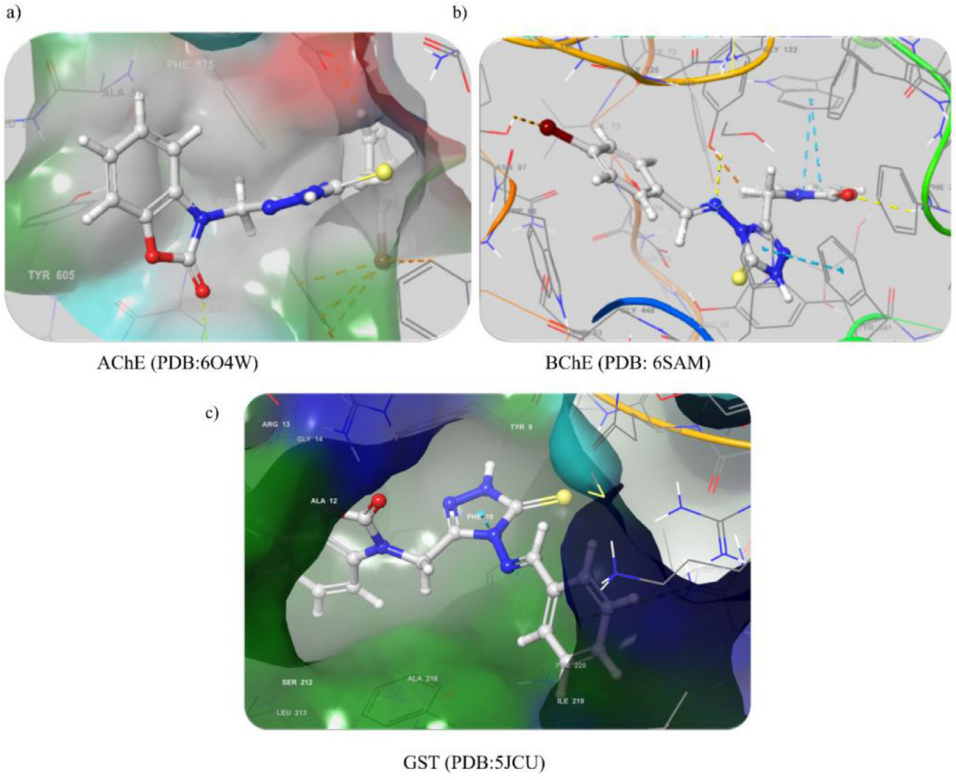


**Fig. 2.** High resulition 3D crystal structures of proteins with the interactive regions. **a)** AChE (Resolution: 2.35 Å), **b)** BChE (Resolution: 2.50 Å) **c)** GST (Resolution: 1.93 Å).

On the other hand, it can be shown the observed peaks that for p-cymene group protons between 5.26-5.47 ppm (4H d, Ru-$C_6\boldsymbol{H}_4$), 2.99-3.02 ppm (1H h, Ru-$C_6H_4C\boldsymbol{H}(CH_3)_2$, 2.26-2.31 ppm (3H s, Ru-$C_6H_4C\boldsymbol{H}_3$), and 1.33-1.34 ppm (6H d, Ru-$C_6H_4CH(C\boldsymbol{H}_3)_2$as evidence [41]. Also, the four peaks corresponding to p-cymene carbons appeared between at 83.1-103.8 ppm in $^{13}C$ NMR spectra of Ru(II) complexes [42].

### 3.1.3. Mass spectra

The mass spectrum of [Ru($\eta^6$p-cymene)$LCl_2$] complexes (2a-c and 2e) showed as the ion peak of the cationic complexes at m/z=586.08, 664.49, 664.99, 620.05 respectively for $[M\text{-}2Cl]^{2+}$. Only for Ru(II) complex (2d) found at m/z=709.02 $[M+NH_4]^+$ because ammonium ion was bounded to the molecule during the dissolution of the complex [43].

## 3.2. Determination of enzyme inhibition study

The synthesized ligands (1a-e) and their Ru(II) complex (2a-e) compounds were investigated for their inhibitory activity on AChE, BChE, and GST. Ki and the half-maximal inhibitory concentration ($IC_{50}$) values of the ligand and its complexes were calculated and evaluated for three metabolic enzymes and the molecular docking study was performed. The results derived for the ligand (1a-e) and their complexes (2a-e) against the AChE, BChE, and GST are given in Table 1. 1a compound was found to be the best inhibitor of BChE and its Ki and $IC_{50}$ values were 23.51 μM and 30.14 μM. BChE inhibited by 2d complex with lower Ki (42.81 μM) and $IC_{50}$ (50.46 μM) values when compared with other compounds. For AChE 2c compound was the best inhibitor with 26.87 μM Ki and 35.76 μM $IC_{50}$ values. 2a compound was the weakest inhibitor for the AChE with 47.63 μM Ki and 53.23 μM $IC_{50}$ values. While2a demonstrated very good inhibitory activity against the GST with 33.14 μM Ki and 42.0 μM $IC_{50}$.1c compound showed very week activity against the GST with 51.73 μM Ki and 58.72 μM $IC_{50}$ values.

## 3.3. Computational analysis

Molecular docking is useful for studying the binding mechanism between the ligand-receptor and understanding the interaction of possible binding modes at the molecular level. Here, molecular docking was performed to obtain the preferred binding sites of the ligands with the receptor and to substantially confirm the experimental observations [44-46]. In the study consisting of 5 different Shiff Base Derivatives and 4 enzyme sets, 20 docking results were obtained (Table 1). These ligands were placed in the catalytic active region of the enzyme and the docking results were analyzed based on binding affinity and interaction mode. The halogenated structures at the ortho-position achieved a good binding score with all enzymes relative to the para position. However, as a molecular structure, the best binding affinity score was observed in AChE and BChE enzymes. The interactions of molecules with enzymes are shown in Figs. 3 and 4. These figures show the interactions of ligands (1a-e) with enzymes. The interaction of the Ru(II) complexes (2a-e) could not be obtained due to the very high molecular volume [15,47]. Molecular structural similarity to the natural ligand in protein structure increases this value. Fig. 2 shows the regions where proteins can interact with 3D crystal structures and small molecules (ligands). The dynamics of the protein play an important role in how proteins interact with Shiff base derivatives to form complexes, which can increase or inhibit its biological function. Since AChE is in the binding inner regions of proteins, higher affinity was found compared to other enzymes.

Ligand-receptor docking binding and interaction parameters are listed in Table 2. In the ligands compared to other enzymes, the highest glide score was calculated as -10.183 kcal/mol between compound 1d and AChE. According to the results Glide scores, 1c

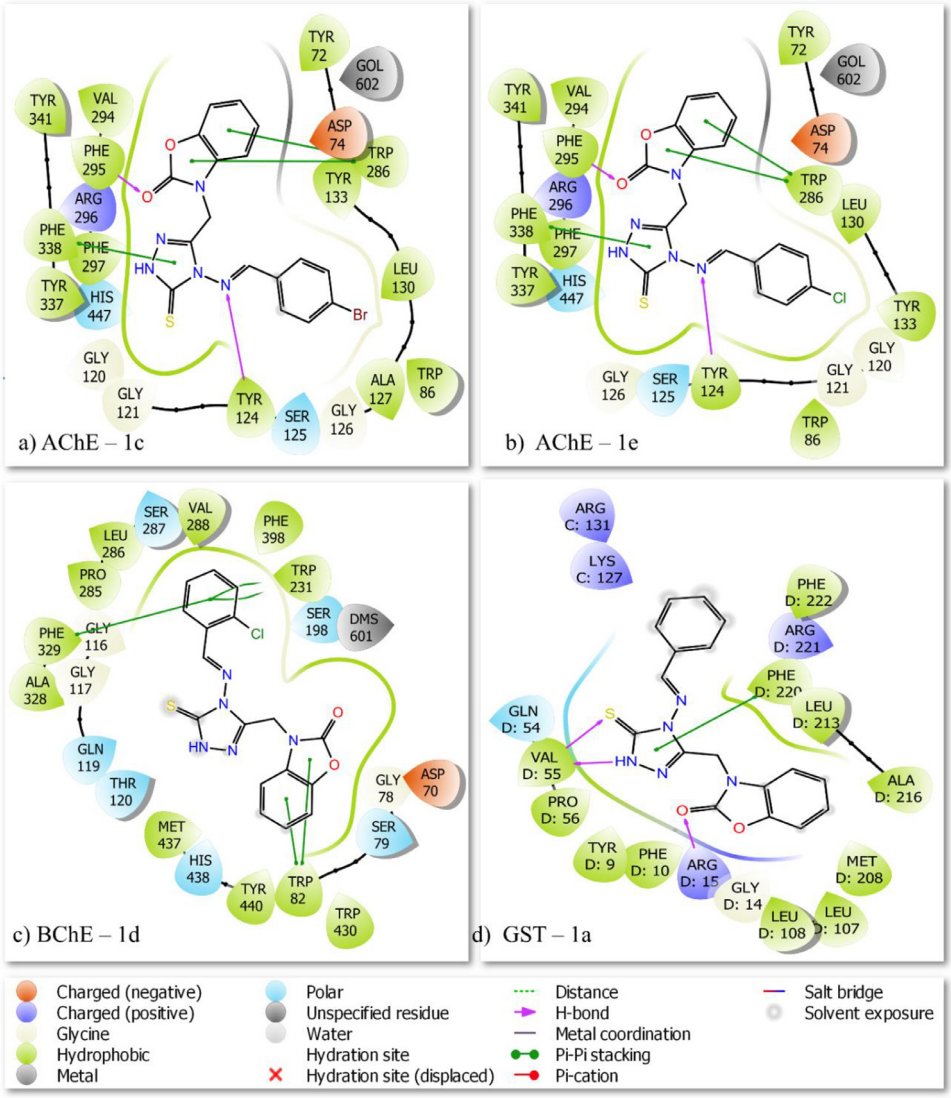


**Fig. 3.** 2D View of the interaction modes between Shiff base derivatives and enzymes, **a) 1c**-AChE, **b)1e**-AChE, **c) 1d-**BChE, **d)1a**-GST.

**Table 2**
Best-binding affinity scores (kcal/mol) of Shiff base derivatives in the catalytic sites of the enzymes.

| **Shiff base derivatives** | **Glide Score** | | |
|---|---|---|---|
| | **AChE** (PDB:6O4W) | **BChE** (PDB: 6SAM) | **GST** (PDB:5JCU) |
| **1a** | -9.933 | -8.513 | -6.097 |
| **1b** | -10.004 | -8.384 | -5.667 |
| **1c** | -9.518 | -7.558 | -5.182 |
| **1d** | -10.183 | -9.111 | -5.936 |
| **1e** | -9.659 | -7.288 | -5.725 |

and 1e exhibited excellent binding affinities to AChE enzymes, as seen in Table 1. The high binding affinity here maybe the reason for the catalytic site selectivity of AChE.In addition to conventional hydrogen bonds, it is another type of hydrogen bond in which $\pi$-systems (especially aromatic rings) play the role of proton acceptors. This type of hydrogen bonding is important in understanding biochemical processes such as hydrophobic interactions in protein, ligand-protein interactions [48,49]. $\pi$ -$\pi$ stacking, unlike a single covalent bond with an energy of more than 47.8 kcal, non-covalent interactions were assumed to be much weaker. While it has an energy of between 5.97 and 9.55 kcal(6) for a hydrogen bond, the energies of non-covalent interactions in Table 1 are less than 2.39 kcal. However, these energies are sufficient for binding [48,49]. Inhibitor activity was powerful due to the $\pi$-donor hydrogen bond (PHE 338) and conventional hydrogen bond (TYR 124). Other binding parameters are given in Fig. 3 a-b. Binding scores also provided well results in the interaction of BChE with Schiff bases derivatives and herein the highest score was found to be -9.111 kcal/mol. $\pi$-alkyl is well docked with interactions such as ALA 328, HIS 438, LEU 286, carbon-hydrogen bond TRP 82, DMS 601 (Fig. 3c). Docking of compound 1a with GST gave the best score with 6.097 kcal/mol. Interactions are present such as protein residues, LEU108, LEU 107, and ALA 216 $\pi$-alkyl, ARG 15, VAL 55, conventional hydrogen bond that contributes to binding affinity (Table 3). Other binding parameters are given in Fig. 3d.

After the best pose selection in all ligand-enzyme docking, binding modes were analyzed to understand the inhibition mechanisms. When Fig. 4a is examined, blue-colored surfaces for aromatic ring edges, an orange-colored surface represents the interaction formed on the aromatic ring faces. In Fig. 4 b, d, the ma-

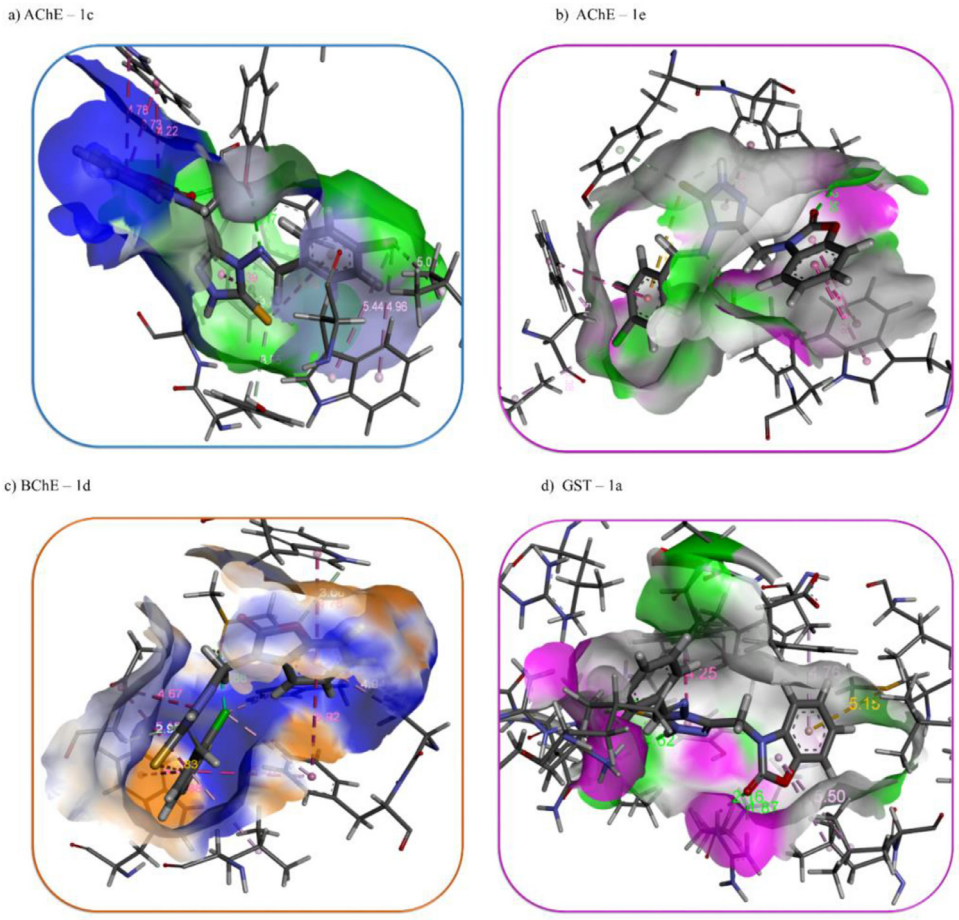


**Fig. 4.** The interaction mode between Shiff base derivatives - the enzymes, 3D View of **a)** the solvent accessibility interaction surface on **1c-AChEb)** the hydrogen bonds donor/acceptor surface on **1e**-AChE, **c)** the aromatic interaction surface on **1d-**BChE, **d)** the hydrogen bonds donor/acceptor surface on **1a**-GST.

**Table 3**
The parameters of the interaction modes between Shiff base derivatives and enzymes, **a) 1c**-AChE, **b)1e**-AChE, **c)1d-**BChE, **d)1a**-GST.

| | AChE - 1c | | AChE - 1e | | BChE-1d | | GST-1a | |
|---|---|---|---|---|---|---|---|---|
| Important interactions | Residues | Bond Length (Å) | Residues | Bond Length (Å) | Residues | Bond Length (Å) | Residues | Bond Length (Å) |
| Conventional Hydrogen Bond | TYR 124-N<br>PHE 295-O | 2.17<br>2.52 | TYR 124-NPHE 295-O | 2.22<br>2.50 | | | ARG 15-O<br>VAL 55-S VAL 55-H | 1.87-2.16,<br>2.72<br>2.62 |
| Pi-Donor Hydrogen Bond | PHE 338-S | 3.78 | | | | | | |
| Pi- Sulfur | TYR 337-S | 3.55 | TYR 337-S | 3.55 | | | MET 208 | 5.15 |
| Pi-Pi stacked | TRP 286,<br>PHE 338 | 3.73, 4.70<br>5.76 | TRP 286<br>PHE 338 TRP 86 –Cl TRP 86 -Ar | 3.73,<br>4.78<br>5.76<br>5.07<br>4.93 | DMS 601-Cl | 2.88 | PHE 220 | 4.25 |
| Pi- Alkyl | LEU 130 | 5.05 | LEU 130-Cl | 5.38 | ALA 328,<br>HIS 438,<br>LEU 286,<br>PHE 329 | 4.94<br>4.38<br>4.83<br>4.78 | LEU 108 LEU 107 ALA 216 | 5.50<br>5.44<br>4.75 |
| Pi-Donor Hydrogen Bond | | | PHE 338 –S | 3.78 | | | | |
| Pi-Pi T-Shaped | | | | | TRP 231<br>PHE 329 | 4.88,4.96,<br>4.78,5.28 | | |
| CarbonHydrogen Bond | | | | | TRP 82 DMS 601 | 3.06<br>2.59,3.10 | | |
| Pi – Lone Pair | | | | | GLY 116 | 4.67,5.16 | | |

genta surfaces in hydrogen bonds represent the donor group, and in green the acceptors. In Fig. 4c, the solvent accessibility of the receptor residues creates a colored surface that decreases from blue to green.

## 4. Conclusion

Herein, [Ru($\eta^6$-p-cymene)$LCl_2$] complexes (2a-e) of Shiff base derivatives of 3-[(4-amino-5-thioxo-1,2,4-triazole-3-yl)methyl]-2(3H)-benzoxazolone ligands (1a-e) were synthesized in very short reaction times and very good yields. The novel synthesized complex structures of ligands were illuminated by spectroscopic methods and elemental analysis. *In vitro* and *in silico* study was used to evaluate the inhibition mechanism of the compounds against the AChE, BChE, and GST enzyme. When compared to standard tacrine it is possible to say the synthesized molecules have significant inhibition effects against the enzymes used.. 1a, 2a, 2c compounds were observed to be the best inhibitors relatively. Both 1a and 2a showed good inhibition effects against the BChE. Inhibition properties of the compounds could be attributed to the contribution of donor atoms of the 1,2,4-triazole group, 2(3H)-benzoxazolone group, and (-CH=N) imine group of the ligands. However, further in vitro and in vivo pharmacological researches need to illuminate the biological activities of these derivatives.

## Declaration of Competing Interest

There are no conflicts to declare.

## Acknowledgments

We appreciate the Catalysis Research and Application Center Inonu University (for analyses of $^1$H NMR and $^{13}$C NMR spectra), Faculty of Pharmacy Department of Pharmaceutical Chemistry Gazi University (for mass spectra), and Tunceli Vocational School, Department of Chemistry and Chemical Process Technologies Munzur University (for FT-IR spectra). The enzyme inhibition study was carried out in Iğdır University Research Laboratory Application and Research Center (ALUM) in Turkey.

## References

[1] H.L. Singh, S. Varshney, A. Varshney, Organotin (IV) complexes of biologically active Schiff bases derived from heterocyclic ketones and sulpha drugs, Appl. Organomet. Chem. 13 (9) (1999) 637–641.
[2] J. Losada, I. Del Peso, L. Beyer, Electrochemical and spectroelectrochemical properties of copper (II) Schiff-base complexes, Inorganica Chimica Acta 321 (1-2) (2001) 107–115.
[3] M. Bingöl, N. Turan, Schiff base and metal (II) complexes containing thiophene-3-carboxylate: Synthesis, characterization and antioxidant activities, J. Mol. Struct. 1205 (2020) 127542.
[4] S.J. Flora, V. Pachauri, Chelation in metal intoxication, Int. J. Environ. Res. Public Health 7 (7) (2010) 2745–2788.
[5] R.G. Mohamed, F.M. Elantabli, A.A.A. Aziz, H. Moustafa, S.M. El-Medani, Synthesis, characterization, NLO properties, antimicrobial, CT-DNA binding and DFT modeling of Ni (II), Pd (II), Pt (II), Mo (IV) and Ru (I) complexes with NOS Schiff base, J. Mol. Struct. 1176 (2019) 501–514.
[6] M.F. Saglam, M. Bingul, E. Şenkuytu, M. Boga, Y. Zorlu, H. Kandemir, I.F. Sengul, Synthesis, characterization, UV–Vis absorption and cholinesterase inhibition properties of bis-indolyl imine ligand systems, J. Mol. Struct. (2020) 128308.
[7] S.U. Cicekli, T. Onkol, S. Ozgen, M.F. Sahin, Schiff bases of 3-[(4-amino-5-thioxo-1, 2, 4-triazole-3-yl) methyl] 2 (3h) benzoxazolonederivatives. synthesis and biological activity, Rev. Roum. Chim. 57 (3) (2012) 187–195.
[8] Z. Soyer, B. Eraç, Evaluation of antimicrobial activities of some 2 (3H)-benzoxazolone derivatives, FABAD J. Pharma. Sci. 32 (4) (2007) 167.
[9] P. Taslimi, K. Turhan, F. Türkan, H.S. Karaman, Z. Turgut, I. Gulcin, Cholinesterases, $\alpha$-glycosidase, and carbonic anhydrase inhibition properties of 1H-pyrazolo [1, 2-b] phthalazine-5, 10-dione derivatives: Synthetic analogues for the treatment of Alzheimer's disease and diabetes mellitus, Bioorg. Chem. 97 (2020) 103647.
[10] M. Durgun, C. Türkeş, M. Işık, Y. Demir, A. Saklı, A. Kuru, A. Güzel, Ş. Beydemir, S. Akocak, S.M. Osman, Synthesis, characterisation, biological evaluation and in silico studies of sulphonamide Schiff bases, J. Enzyme Inhib. Med. Chem. 35 (1) (2020) 950–962.
[11] S. Bayindir, C. Caglayan, M. Karaman, İ. Gülcin, The green synthesis and molecular docking of novel N-substituted rhodanines as effective inhibitors for carbonic anhydrase and acetylcholinesterase enzymes, Bioorg. Chem. 90 (2019) 103096.
[12] J. Zhu, H. Yang, Y. Chen, H. Lin, Q. Li, J. Mo, Y. Bian, Y. Pei, H. Sun, Synthesis, pharmacology and molecular docking on multifunctional tacrine-ferulic acid hybrids as cholinesterase inhibitors against Alzheimer's disease, J. Enzyme Inhib. Med. Chem. 33 (1) (2018) 496–506.
[13] M. Boztas, P. Taslimi, M.A. Yavari, I. Gulcin, E. Sahin, A. Menzek, Synthesis and biological evaluation of bromophenol derivatives with cyclopropyl moiety: Ring opening of cyclopropane with monoester, Bioorg. Chem. 89 (2019) 103017.
[14] M.B. Colovic, D.Z. Krstic, T.D. Lazarevic-Pasti, A.M. Bondzic, V.M. Vasic, Acetylcholinesterase inhibitors: pharmacology and toxicology, Curr. Neuropharmacol. 11 (3) (2013) 315–335.
[15] F. Türkan, P. Taslimi, S.M. Abdalrazaq, A. Aras, Y. Erden, H.U. Celebioglu, B. Tuzun, M.S. Ağırtaş, İ. Gülçin, Determination of anticancer properties and inhibitory effects of some metabolic enzymes including acetylcholinesterase, butyrylcholinesterase, alpha glycosidase of some compounds with molecular docking study, J. Biomol. Struct. Dyn. (just-accepted) (2020) 1–17.
[16] P. Masson, E. Carletti, F. Nachon, Structure, activities and biomedical applications of human butyrylcholinesterase, Protein Peptide Lett.16 (10) (2009) 1215–1224.
[17] M.-M. Mesulam, A. Guillozet, P. Shaw, A. Levey, E. Duysen, O. Lockridge, Acetylcholinesterase knockouts establish central cholinergic pathways and can use butyrylcholinesterase to hydrolyze acetylcholine, Neuroscience 110 (4) (2002) 627–639.
[18] R.E. Selim, H.H. Ahmed, S.H. Abd-Allah, G.M. Sabry, R.E. Hassan, W.K. Khalil, N.S. Abouhashem, Mesenchymal stem cells: a promising therapeutic tool for acute kidney injury, Appl. Biochem. Biotechnol. 189 (1) (2019) 284–304.
[19] N. Verma, A. Yadav, S. Bal, R. Gupta, N. Aggarwal, In vitro studies on ameliorative effects of limonene on cadmium-induced genotoxicity in cultured human peripheral blood lymphocytes, Appl. Biochem. Biotechnol. 187 (4) (2019) 1384–1397.
[20] N. Allocati, M. Masulli, C. Di Ilio, L. Federici, Glutathione transferases: substrates, inihibitors and pro-drugs in cancer and neurodegenerative diseases, Oncogenesis 7 (1) (2018) 1–15.
[21] S. Boy, F. Türkan, M. Beytur, A. Aras, O. Akyıldırım, H.S. Karaman, H. Yüksek, Synthesis, design, and assessment of novel morpholine-derived Mannich bases as multifunctional agents for the potential enzyme inhibitory properties including docking study, Bioorg. Chem. (2020) 104524.
[22] F. Turkan, Z. Huyut, P. Taslimi, I. Gulcin, The effects of some antibiotics from cephalosporin groups on the acetylcholinesterase and butyrylcholinesterase enzymes activities in different tissues of rats, Arch. Physiol. Biochem. 125 (1) (2019) 12–18.
[23] P. Taslimi, Y. Erden, S. Mamedov, L. Zeynalova, N. Ladokhina, R. Tas, B. Tuzun, A. Sujayev, N. Sadeghian, S.H. Alwasel, The biological activities, molecular docking studies, and anticancer effects of 1-arylsuphonylpyrazole derivatives, J. Biomol. Struct. Dyn. (just-accepted) (2020) 1–20.
[24] P. Taslimi, A. Sujayev, F. Turkan, E. Garibov, Z. Huyut, V. Farzaliyev, S. Mamedova, İ. Gulçin, Synthesis and investigation of the conversion reactions of pyrimidine-thiones with nucleophilic reagent and evaluation of their acetylcholinesterase, carbonic anhydrase inhibition, and antioxidant activities, J. Biochem. Mol. Toxicol. 32 (2) (2018) e22019.
[25] F. Türkan, Z. Huyut, P. Taslimi, İ. Gülçin, The effects of some antibiotics from cephalosporin groups on the acetylcholinesterase and butyrylcholinesterase enzymes activities in different tissues of rats, Arch. Physiol. Biochem. (2018) 1–7.
[26] H.E. Aslan, Y. Demir, M.S. Özaslan, F. Türkan, Ş. Beydemir, Ö.I. Küfrevioğlu, The behavior of some chalcones on acetylcholinesterase and carbonic anhydrase activity, Drug Chem. Toxicol. (2018) 1–7.
[27] O. Gerlits, K.-Y. Ho, X. Cheng, D. Blumenthal, P. Taylor, A. Kovalevsky, Z. Radić, A new crystal form of human acetylcholinesterase for exploratory room-temperature crystallography studies, Chem.-Biol. Interact.309 (2019) 108698.
[28] U. Košak, N. Strašek, D. Knez, M. Jukič, S. Žakelj, A. Zahirović, A. Pišlar, X. Brazzolotto, F. Nachon, J. Kos, S. Gobec, N-alkylpiperidine carbamates as potential anti-Alzheimer's agents, Eur. J. Med. Chem.197 (2020) 112282.
[29] V. Kumari, M.A. Dyba, R.J. Holland, Y.-H. Liang, S.V. Singh, X. Ji, Irreversible Inhibition of Glutathione S-Transferase by Phenethyl Isothiocyanate (PEITC), a Dietary Cancer Chemopreventive Phytochemical, PLOS ONE 11 (9) (2016) e0163821.
[30] D. Biovia, H. Berman, J. Westbrook, Z. Feng, G. Gilliland, T. Bhat, T.J.T.J.o.C.P. Richmond, Dassault Systèmes BIOVIA, Discovery Studio Visualizer, v. 17.2, Dassault Systèmes, San Diego, 2016 10 (2000) 0021-9991.
[31] E. Praveenkumar, N. Gurrapu, P. Kumar Kolluri, V. Yerragunta, B. Reddy Kunduru, N.J.P. Subhashini, Synthesis, anti-diabetic evaluation and molecular docking studies of 4-(1-aryl-1H-1, 2, 3-triazol-4-yl)-1,4-dihydropyridine derivatives as novel 11-$\beta$ hydroxysteroid dehydrogenase-1 (11$\beta$-HSD1) inhibitors, Bioorg. Chem.90 (2019) 103056.

[32] N.J.P. Subhashini, E. Praveen Kumar, N. Gurrapu, V. Yerragunta, Design and synthesis of imidazolo-1, 2,3-triazoles hybrid compounds by microwave-assisted method: Evaluation as an antioxidant and antimicrobial agents and molecular docking studies, J. Mol. Struct.1180 (2019) 618–628.
[33] M. Taha, M.S. Baharudin, N.H. Ismail, S. Imran, M.N. Khan, F. Rahim, M. Selvaraj, S. Chigurupati, M. Nawaz, F. Qureshi, S. Vijayabalan, Synthesis, $\alpha$-amylase inhibitory potential and molecular docking study of indole derivatives, Bioorg. Chem.80 (2018) 36–42.
[34] D.S.Biovia, Discovery studio modeling environment, Release, 2017.
[35] A. Allen, C. Senoff, Preparation and infrared spectra of some ammine complexes of ruthenium (II) and ruthenium (III), Can. J. Chem. 45 (12) (1967) 1337–1341.
[36] A.J. Abdulghani, N.M. Alabidy, Synthesis and biological activity study of new Schiff and Mannich base ligands derived from isatin and 3-amino-1, 2, 4-triazole and their metal complexes, J. Chem. Chem. Eng. 5 (1) (2011).
[37] R. Gup, B. Kırkan, Synthesis and spectroscopic studies of copper (II) and nickel (II) complexes containing hydrazonic ligands and heterocyclic coligand, Spectrochim. Acta Part A Mol. Biomol. Spectros.62 (4–5) (2005) 1188–1195.
[38] H. Ünver, F. Yilmaz, Synthesis of new Rh (I) and Ru (III) complexes and investigation of their catalytic activities on olefin hydrogenation in green reaction media, 3rd Int. Conf. New Trend Chem. (2017) 114.
[39] A.E.-M.M. Ramadan, I.M. El-Mehasseb, R.M. Issa, Synthesis, characterization and superoxide dismutase mimetic activity of ruthenium (III) oxime complexes, Trans. Metal Chem.22 (6) (1997) 529–534.
[40] K. Ayşe, Ö. KARAGÜZEL, K. AYDİNŞAKİR, S. KAZAZ, A. ÖZÇELİK, Türkiye'de doğal olarak yetişen bazı gypsophila (Gypsophila sp.) türlerinin süs bitkisi olarak kullanım olanakları, Derim 29 (1) (2012) 37–47.
[41] F.A. Egbewande, L.E. Paul, B. Therrien, J. Furrer, Synthesis, Characterization and Cytotoxicity of ($\eta$6-p-cymene) ruthenium (II) Complexes of $\alpha$-Amino Acids, Eur. J. Inorg. Chem. 2014 (7) (2014) 1174–1184.
[42] T. Seckin, S. Köytepe, B. Çetinkaya, İ. Özdemir, B. Yigit, Synthesis and properties of novel polyimides from dichloro (1, 3-p-dimethylaminobenzylimidazolidine-2-ylidene) p-cymene ruthenium (II), Des. Monomers Polym. 6 (2) (2003) 175–185.
[43] N. Turan, B. Gündüz, H. Körkoca, R. Adigüzel, N. Çolak, K. Buldurun, Study of structure and spectral characteristics of the Zinc (II) and Copper (II) complexes with 5, 5-Dimethyl-2-(2-(3-nitrophenyl) hydrazono) cyclohexane-1, 3-dione and their effects on optical properties and the developing of the energy band gap and investigation of antibacterial activity, J. Mexican Chem. Soc.58 (1) (2014) 65–75.
[44] Q. Cao, Y. Huang, Q.-F. Zhu, M. Song, S. Xiong, A. Manyande, H. Du, The mechanism of chlorogenic acid inhibits lipid oxidation: An investigation using multi-spectroscopic methods and molecular docking, Food Chem. (2020) 127528.
[45] P. Śledź, A. Caflisch, Protein structure-based drug design: from docking to molecular dynamics, Curr. Opin. Struct. Biol.48 (2018) 93–102.
[46] J. Guo, M.M. Hurley, J.B. Wright, G.H.J.J.o.m.c. Lushington, A docking score function for estimating ligand– protein interactions: Application to acetylcholinesterase inhibition 47 (22) (2004) 5492–5500.
[47] K. Sayin, A. Üngördü, Investigations of structural, spectral and electronic properties of enrofloxacin and boron complexes via quantum chemical calculation and molecular docking, Spectrochim. Acta Part A Mol. Biomol. Spectros.220 (2019) 117102.
[48] A.R. Nekoei, M. Vatanparast, $\pi$-Hydrogen bonding and aromaticity: a systematic interplay study, Phys. Chem. Chem. Phys.21 (2) (2019) 623–630.
[49] J.-H. Deng, J. Luo, Y.-L. Mao, S. Lai, Y.-N. Gong, D.-C. Zhong, T.-B. Lu, $\pi$-$\pi$ stacking interactions, Non-negligible forces for stabilizing porous supramolecular frameworks 6 (2) (2020) eaax9976.